

# The Dirac fermion of a monopole pair (MP) model

Samuel. P. Yuguru<sup>1</sup>

1. Chemistry Department, School of Natural and Physical Sciences, University of Papua New Guinea, P. O. Box 320, Waigani Campus, National Capital District 134, Papua New Guinea, Tel. : +675 326 7102; Fax. : +675 326 0369; Email address: [samuel.yuguru@upng.ac.pg](mailto:samuel.yuguru@upng.ac.pg).

## Abstract

The electron of magnetic spin  $-1/2$  is a Dirac fermion of a complex four-component spinor field. Though it is effectively addressed by relativistic quantum field theory, an intuitive form of the fermion still remains lacking. In this novel undertaking, the fermion is examined within the boundary posed by a recently proposed MP model of a hydrogen atom into 4D space-time. Such unorthodox process conceptually transforms the electron to the four-component spinor of non-abelian in both Euclidean and Minkowski space-times. Supplemented by several postulates, the relativistic and non-relativistic applications of the model are explored from an alternative perspective. The outcomes have important implications towards defining the spin-orbit coupling of particles from external light interactions. These findings, if considered could consolidate properly the fundamentals of the quantum state of matter from an alternative perspective using quantum field theory application and they warrant further investigations.

**Keywords:** Dirac fermion, magnetic spin, 4D space-time, spin-orbit coupling

## 1. Introduction

At the fundamental level of matter, particles are described by wave-particle duality, charges and their spin property [1, 2]. These properties are revealed from light interactions and are pursued by the application of relativistic quantum field theory (QFT) [3–6]. The theory of special relativity defines lightspeed,  $c$  to be constant in a vacuum and the rest mass,  $m$  of particles,  $m = E/c^2$  with  $E$  equal to energy[3, 4]. By definition, the particle-like property of light waves is massless photons possessing spin 1 of neutral charge. Any differences to the spin, charge and mass-energy equivalence provide the inherent properties of the particles at the fundamental level and this is termed causality [1, 2]. Based on QFT, particles are considered to be fields permeating space at less than lightspeed, where there is a level of indetermination towards unveiling their charge and spin property, while the wave-particle characteristic is depended on the instrumental set-up [7, 8]. Such definition counteracts the deterministic viewpoint of non-relativistic Schrödinger's electron field wave function,  $\psi$ , which is extremely useful in describing precisely the probability of future events for a lone particle like an electron in orbit of the atom [9]. First, it does not account for the spin property of the particles. Second,  $\psi$  is classically applied to physical waves such as for the water waves. Thus, it is difficult to imagine wavy form of particles freely permeating space without interactions and this somehow collapses to a point at observation [10].

At the atomic state, the energy is radiated in discrete energy forms in infinitesimal steps of Planck's radiation,  $\pm h$ . Such interpretation is consistent with observations except for the

resistive nature of proton decay [11]. Despite this set-back, the preferred quest is to make non-relativistic equations become relativistic due to the shared properties of both matter and light at the fundamental level as mentioned above.

Beginning with Klein-Gordon equation [12], the energy and momentum operators of Schrödinger equation,

$$\hat{E} = i\hbar \frac{\partial}{\partial t}, \quad \hat{p} = -i\hbar \nabla, \quad (1)$$

are adapted in the expression,

$$\left( \hbar^2 \frac{\partial^2}{\partial t^2} - c^2 \hbar^2 \nabla^2 + m^2 c^4 \right) \psi(t, \bar{x}) = 0. \quad (2)$$

Equation 2 incorporates special relativity,  $E^2 = p^2 c^2 + m^2 c^4$  for mass-energy equivalence,  $\nabla$  is the del operator in 3D space,  $\hbar$  is reduced Planck constant and  $i$  is an imaginary number,  $i = \sqrt{-1}$ . Only one component is considered in Equation 2 and it does not take into account the negative energy contribution from antimatter. In contrast, the Hamiltonian operator,  $\hat{H}$  of Dirac equation [13] for a free particle is,

$$\hat{H}\psi = (-i\nabla \cdot \boldsymbol{\alpha} + m\beta)\psi. \quad (3)$$

The  $\psi$  has four-components of fields,  $i$  with vectors of momentum,  $\nabla$  and gamma matrices,  $\alpha, \beta$  represent Pauli matrices and unitarity with  $m$  equal to particle mass. The concept is akin to,  $e^+ e^-$

→  $2\gamma$ , where the electron annihilates with its antimatter to produce two gamma rays. Antimatter existence is observed in Stern-Gerlach experiment and positron from cosmic rays. While the relativistic rest mass is easy to grasp, how fermions acquire mass other than Higgs field remains yet to be solved at a satisfactory level [14]. But perhaps, the most intriguing dilemma is offered by the magnetic spin  $\pm 1/2$  of the electron and how this translates to a Dirac fermion of a four-component spinor field. Such a case remains a very complex topic, whose intuitiveness in terms of a proper physical entity remains lacking and it is often described either by the so-called Dirac belt trick [5] or Balinese cup trick [6]. In this novel undertaking, the electron is examined within the boundary posed by a recently proposed MP model of 4D space-time of a hydrogen atom [15]. With this process, the transition of the electron to a Dirac fermion is unveiled. Supplemented by a number of postulates, the fermion's relationships to both relativistic and non-relativistic aspects of the spin property are examined from an alternative perspective. The outcomes have important implications towards defining the spin-orbit coupling of particles from external light interactions. If considered, these findings could consolidate properly the fundamentals of the quantum state of matter from an alternative perspective using QFT application and they warrant further investigations.

## 2. The wrong turn with QFT interpretations

Yukawa definition for the relativistic range of interaction,  $R = \hbar/mc$  adapts the uncertainty principle [16]. This is incorporated into the Yang-Mills theory of the non-abelian Standard Model of particles, where relativistic mass,  $m = 0$  sustains unitarity and gauge invariance [17]

90 such as for quark confinement in which case,  $R$  becomes infinite comparable to the property of  
91 asymptotic freedom [18]. Similarly,  $m \neq 0$  draws divergent terms to the Fourier Transform  
92 integral,  $\int d^4k$  with  $k$  equal to 4<sup>th</sup> dimensional variable [19]. For Dirac fermion of four-  
93 component spinor field, renormalization is assumed by particle self-interaction with exchanges  
94 of virtual photons delineated to Feynman path integral diagrams [3, 4]. The SM lagrangian  
95 resolves the infinite high-order terms, where transition from  $m = 0$  to  $m \neq 0$  is accounted for by  
96 dynamic chiral symmetry breaking like the Higgs scalar field [19, 20],  $\Phi$  of quartic self-  
97 interacting terms. The theory has seen tremendous success, where it ably accounts for all  
98 observations made so far into the electroweak force interactions. However, the notion of matter  
99 existing either as wave or particle at the fundamental level cannot be true for this is depended on  
100 the instrumental setup [7, 8]. Such flawed assumption is adapted by QTF like the SM and it  
101 considers a particle to be a field permeating space and it somehow collapses to a point at  
102 observation. Furthermore, the relativistic mass-energy equivalence,  $E = mc^2$  is accorded to the  
103 particle travelling near the speed of light. These intuitions are at odds with the fermions as the  
104 building blocks of matter with their spin property defined by Pauli exclusion principle. For they  
105 cannot be converted to energy for it would mean the collapse and disintegration of matter. Thus,  
106 Wolfgang Pauli was aghast by Yang-Mills preposition of zero mass for it produces infinite terms  
107 to relativistic mass [21]. The Higgs boson does not resolve this problem for its resistive nature to  
108 decay into observable supersymmetry partners of fermions and bosons offers the hierarchy  
109 problem [22]. So to draw back on the Copenhagen interpretation of quantum mechanics [23], an  
110 elementary charge particle like electron possesses superposition states of spin  $\pm 1/2$ , and this  
111 offers a level of indeterminacy at observations. Similarly, its momentum and position cannot be  
112 constrained simultaneously. Its evolution with time is described very well by Schrödinger  $\psi$

without accounting for the spin property [9]. How this is physically transformed to a Dirac fermion is conceptualized in this study and is supplemented by several postulates pertinent to the tenets of physics. From this basis, the electron’s relationships to both relativistic and non-relativistic aspects are explored from an alternative perspective.

### 3. Conceptualization process of the MP model

An alternative version of how the electron is converted to a Dirac fermion of four-component spinor in non-abelian Euclidean space-time is presented in Fig. 1a. In Fig. 1b, the fermion of spin  $\pm 1/2$  in superposition states of Minkowski space-time is offered. From these illustrations, a number of postulates can be drawn from the first principle of space-time.

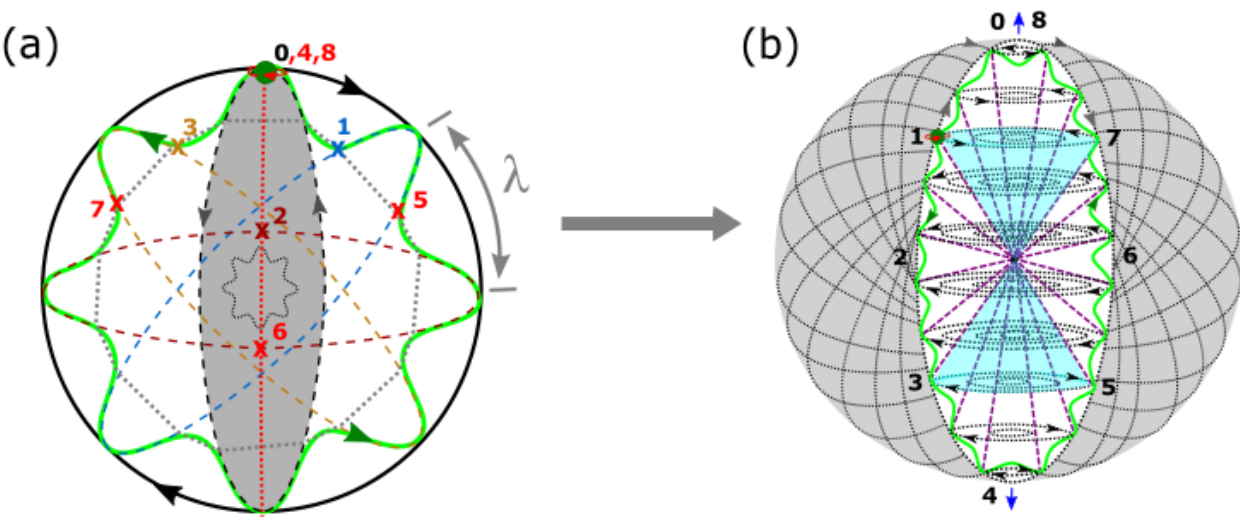


**Figure 1. The MP model [15].** (a) In 2D space, a spinning electron’s (green dot) orbit of time reversal due to gravity is transformed to an elliptic MP field (grey area). Its precession of a clock face (black and grey arrows) generates a 4D space-time. The circular **E** appears to be a straight line (red dotted) and this

perpendicularly dissects the monopole field to generate its dipole moment. (b) The MP field (white area) at position 1 is projected along the vertical axis for an electron cloud model. Minkowski space-time is applicable to an *internal observer* positioned at the center. The pairings of 1, 5 and 3, 7 of the Bohr orbits (BOs) (a) translate to angular momentum and these combine to produce a pair of light-cones (navy colored). Orthogonal projection of chirality,  $\frac{1}{2}(1 \pm i\gamma^0\gamma^1\gamma^2\gamma^3)$  with respect to the electron's path is reduced to spin,  $\frac{1}{2}(1 \pm i\gamma^1\gamma^3)$  along BOs with the superscripts equal to Dirac matrices [3, 4] (*Postulate 1*). Inversion of symmetry through the center violates parity, whereas chirality and time reversal symmetry are sustained. In Hilbert space, the spin angular momentum (purple dotted lines) of the orbit is projected towards singularity at the center. Its outward projection relates to the precession of the overarching MP field. **E** of a straight path is assumed by the arrow of time of a light-cone in asymmetry of unidirectional and it translates to a magnetic dipole moment (blue arrows) of the MP field. In this way, Schrödinger  $\psi$  is transformed to a Dirac fermion of a four-component spinor field,  $i\gamma^0\gamma^1\gamma^2\gamma^3$ .

- 1) A lone electron in orbit of the MP model is likened to Bohr model of the hydrogen atom (Fig. 1a). Its circular orbit is transformed to an elliptic MP field of **B** and this is dissected perpendicularly by a circular **E** of a straight path of a dipole moment. Precession of the MP field of a clock face generates a 4D space-time. The electron's orbit of time reversal due Einsteinian gravity [15] is quantized along Bohr orbits (BOs) in degeneracy into  $n$ -dimensions. The cyclic BO in Euclidean space-time (e.g., positions 1 and 5 in Fig. 1a) is somehow transformed to angular momentum in Minkowski space-time (Fig. 1b). Such pairings of positions 1, 5 and 3, 7 offer both local realism and entanglement of electron-positron pair in violation of lightspeed of spherical rotation at  $360^\circ$  (e.g., Fig. 2). The spacing between the BOs of  $n$ -dimensions is defined by  $h$  with unitarity,  $\lambda$  sustained. Its excitation from external light interaction assumes,  $E = nh\nu$ , whereas the probability of locating the electron of Schrödinger  $\psi$  is defined by De Broglie relationship,  $\lambda = h/p$

(e.g., Fig. 3). Multiple MP fields are expected for electrons distribution in multielectron atoms.

- 2) The orthogonal relationship between  $\mathbf{E}$  and  $\mathbf{B}$  by reciprocity transforms the precession of the MP field of a clock face to a straight path dissecting a spherical  $\mathbf{E}$  (e.g., Fig. 4). The electron path is composed of both  $u$ - and  $v$ -type particle-like properties in Hilbert space. Parity transformation from positions 0 to 4 and then 4 to 8 of  $720^\circ$  rotation appears invariant to the electron path of a straight line (Fig. 4). In Fig. 2, a positive helicity or right-handedness for spin in accordance with precession of a clockwise direction is envisioned for the electron. Negative helicity or left-handedness is assigned to the spin of anticlockwise direction to precession for a positron. The electron assumes a chiral

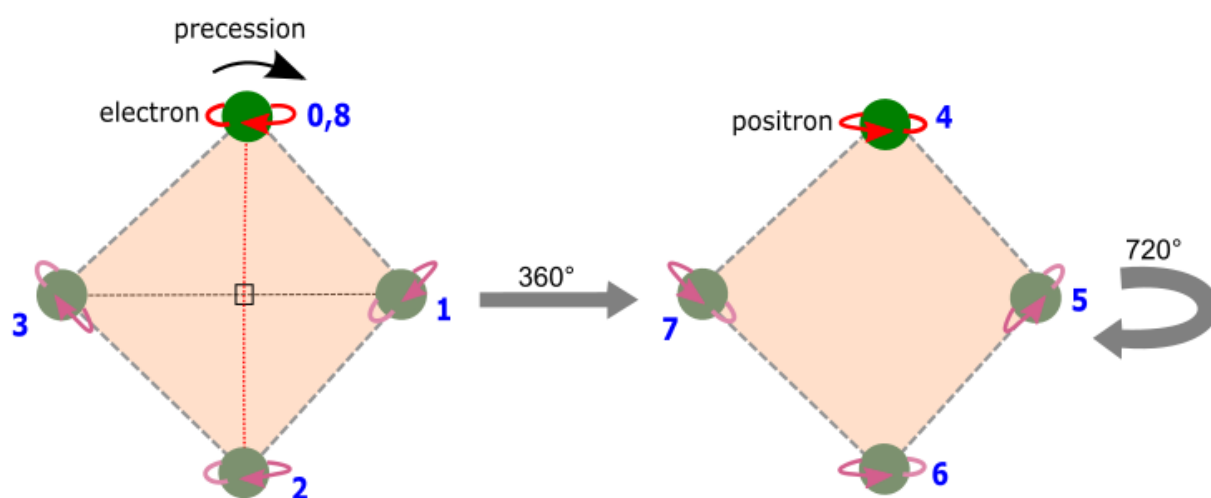


**Figure 2. Electron-positron pair.** To an external observer at an inertia frame of reference, the electron pops in and out of existence at positions, 0, 1, 2, 3 (Fig. 1a) for a  $360^\circ$  rotation to generate a positron at position, 4 of maximum twists provided by the torque of the BOs. In this case, the spin is of anticlockwise direction to the precession of the MP field (black curve arrow) of a clock face. The process is attained at a classical rotation of  $180^\circ$  of a hemisphere (Fig. 1a). The unfolding process at  $720^\circ$  rotation (i.e.,  $360^\circ$



classical rotation) towards position 8 or 0 restores the electron to its original state. The area defined by the shift in the electron's positions is of non-abelian Euclidean lattice. Where positions 1 and 3 converge at either position 0 or 2 on a surface of a sphere indicates non-Euclidean space. This is applicable to the equivalence principle of general relativity [24].

symmetry and the probability of locating it at any positions from 0 to 8 is Hermitian of the orthogonal relationship,  $P(0 \rightarrow 8) = \int_{\tau} \psi^* \hat{H} \psi d\tau$ , with  $\tau$  equal to time. The unitarity gauge obeys the "natural units",  $\hbar = c = 1$  with the electron's orbit accorded to the Euler's formula,  $e^{i\pi} + I = 0$  for continual precession (e.g., Fig. 3). The electron's position,  $i\hbar$  within a sphere (e.g., Fig. 4) incorporates the uncertainty principle,  $\Delta E \Delta t \geq \hbar/2$  or  $\Delta x \Delta p \geq \hbar/2$  of time invariance.

3) The Dirac four-component spinor,  $\psi = \begin{pmatrix} \psi_0 \\ \psi_1 \\ \psi_2 \\ \psi_3 \end{pmatrix}$  assumes its own antimatter at positions, 0,

1, 2 and 3 in Hilbert space (Fig. 4). By reduction, only two positions  $\psi_1$  and  $\psi_3$  generate the spin,  $\pm 1/2$  property and the pair is linked by a geodesic curve of a closed loop (Fig. 1b). The outcome of the spin is determined by Born's probabilistic interpretation,  $|\psi|^2$ , where the past or future paths of the electron from positions 0 to infinity are not accounted for at observations [3, 4].

4) In a multiverse of the models at a hierarchy of energy scales, the procession ensues in the following manner, nucleus  $\Rightarrow$  atom  $\Rightarrow$  planet  $\Rightarrow$  star  $\Rightarrow$  galaxy. There is noticeable distinction to matter between the scales such as life on Earth and gluons at the nucleus. However, the underlying structure of fermions in accordance with Pauli exclusion principle is possibly dictated by the MP model of electromagnetic field, in which case,

fine-tuning appears to be heuristic in principle (e.g., Fig. 5a and b). So the relationship of the electron to an atom is comparable to satellite to planet, planet to star and possibly star to galaxy. Whether these explanations could accommodate the basic principles of general relativity is open to further discussions. For example, based on Fig. 4 and Fig. 1a, gravitational time dilation is applicable in Hilbert space, gravitational lensing to the shifts in the orthogonal relationship between **E** and **B** of the MP model and perihelion precession to the rotation of the MP field of a clock face.

- 5) If time of a clock face resembles the precession of the MP field into 4D space-time, it would tick faster at the atomic scale with respect to lightspeed of  $360^\circ$  spherical rotation. Linearly, this would transform to a constant speed in a vacuum (e.g., Fig. 6a and b). In this case, entanglement is assumed at  $720^\circ$  rotation for the transformation of the electron path to electron-positron pair (Fig. 2) compared to lightspeed. Local realism is sustained by the electron as an elementary particle. The progression of time towards higher hierarchy of scales in a multiverse is slowed or redshifted consistent with the twin paradox narrative [25]. However, this will present the illusion of the clock ticking faster if the Earth's orbit is of time reversal with respect to precession of its MP field of a clock face to generate an inertia frame of reference at the ground level. Similarly, the observer on Earth would be subject to Mercury's unusual perihelion precession [26] and redshift in the sun's precession about the Milky Way. In this case, the cosmic microwave background of a MP field type and its precession is expected to be considerably redshifted of linear time [13, 27]. Thus, Clausius's conservation of energy for the universe is assumed [28], where entropy is recycled in a multiverse by the application of 2<sup>nd</sup> law of thermodynamics at reduced rate towards a higher hierarchy of scales.

The above postulates based on the transformation of the electron to Dirac fermion are pertinent to the tenets of physics. These provide the basis to explore both relativistic and non-relativistic aspects of the hydrogen atom of a MP model of 4D space-time.

## 4. Non-relativistic aspects of the hydrogen atom

The wave-particle duality of the electron is described by the Bohr model of the hydrogen atom [29] (Fig. 3). Its orbit is considered to be of time reversal due to Einsteinian gravity [15] and is balanced by its transformation to an elliptic MP field with precession of a clock face into 4D space-time (Fig. 1a). This provides an inertia frame of reference on the boundary of the MP field. Its position in 3D space is established by non-relativistic Schrödinger  $\psi$  of spherical polar coordinates,  $\Omega$ ,  $\Phi$ ,  $\theta$  with respect to the Cartesian coordinates,  $x$ ,  $y$ ,  $z$  (Fig. 3). Its angular component is assigned to Bohr orbit and is demarcated by  $\theta$ . A diagonal pair of BOs intersecting at the center encompasses a pair of light-cones in accordance with Minkowski space-time (Fig. 1b). The magnetic momentum is offered by  $\Phi$  within a cylindrical boundary. The radial component into  $n$ -dimension is referenced to the  $z$ -axis. The configurations of  $\psi$  due to the precession of the MP field are defined by  $\Omega$  of a von Neumann entropy state (Fig. 3). The microcanonical ensemble for the entropy,  $S = k \ln \Omega$  is applicable to the model, with  $k$  providing an approximation of the electron transition into space of quantized form with exponential rise in Hilbert space. The precession of the spherical model assumes the integrals [30],

$$\int_0^\infty \int_0^\pi \int_0^{2\pi} f(r) r^2 \sin\theta dr d\theta d\phi = \int_0^\infty f(r) 4\pi r^2 dr. \quad (4)$$

where the polar coordinates for the axes are,  $x = r \sin\theta \cos\phi$ ,  $y = r \sin\theta \sin\phi$  and  $z = r \cos\theta$  (Fig. 3). The shift in the electron's position,  $i\hbar$  obeys the Euler's form,  $\psi^{i\theta} = \cos\theta + i \sin\theta$ . Its evolution with time adheres to the generic non-linear Schrödinger equation,

$$i\hbar \frac{\partial \psi}{\partial t}(x, t) = \hat{H} \psi(x, t). \quad (5)$$

Equation 5 is of first order in space-time and is applicable to Equation 3. It cannot be derived by QFT application. The,  $\psi_{n,l,m,m_s}$  incorporates the quantum parameters of principal quantum

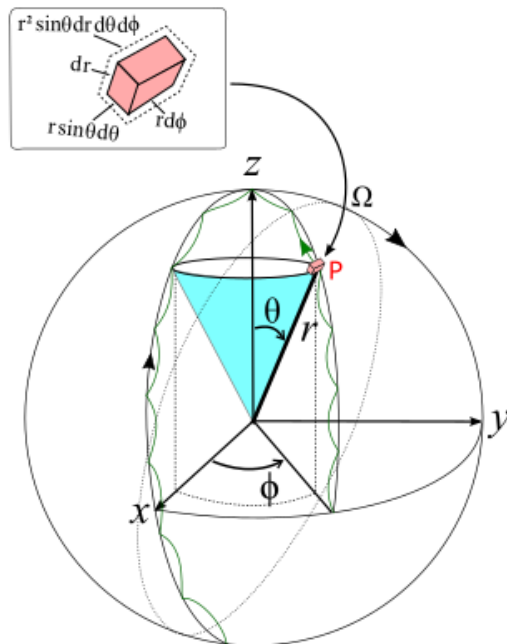


**Figure 3. Deterministic harmonic oscillation (green wavy curve) of Schrödinger  $\psi$  within the MP field.** The electron is considered a physical entity (insert image), where its mass acquisition scenario is attained by the oscillation process. The polar coordinates are referenced to the center. Image modified from ref [30].

number ( $n$ ), angular momentum quantum number ( $l$ ) and magnetic quantum number ( $m$ ). The magnetic spin ( $m_s$ ) in Minkowski space-time offers a level of

indeterminacy (*Postulate 5*) comparable to Schrödinger's cat narrative [31] of superposition of coherent states prior to observation. How

these all align with entanglement, spin-orbit coupling splitting, including generation of linear electromagnetic waves is considered next.

## 5. Relativistic transformation of the hydrogen atom

The electron orbit within the elliptic MP field is envisioned to be a straight path of magnetic field, **B** orthogonal to a cyclic electric field, **E**. Further explanations on the numbered positions are offered in Fig. 1a and b. In Fig. 4, the electron translates to a positron at anticlockwise spin to the precession of a clock face and vice versa (see also Fig. 2). Because position 0 can shift to

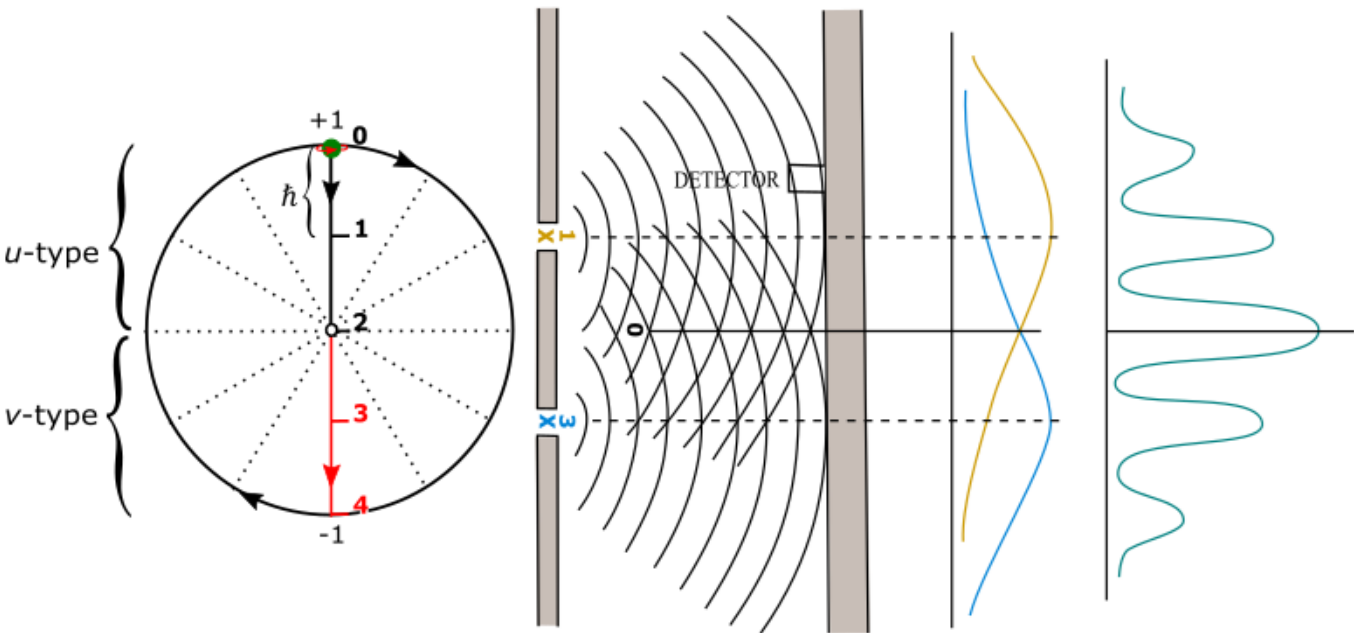


**Figure 4. Wave-particle duality of the electron,  $i\hbar$ .** The fermion (green circle) and its wave property are relatable to the double slit experiment for Born's probabilistic interpretation,  $|\psi|^2$  by decoherence at observation (*Postulate 3*). The  $\pm 1/2$  spins at positions 0 to 4 from the electron's orbit at  $360^\circ$  is provided.

The reversal process from position 4 to 8 or 0 provides superposition states of the spins at  $720^\circ$  rotation. The electron's path constitutes both  $u$ - and  $v$ -type particle-like properties in Hilbert space of the vacuum. Parity transformation is attained through the center to generate polarization,  $\pm 1$  for the qubits 0 and  $\pm 1$ . These interpretations are consistent with the Schrödinger's cat narrative and hence, the wave function collapse scenario. The actual numbered positions from 0 to 8 in repetitive process are offered in Fig. 1a and b.

anywhere on the spherical boundary, this offers both  $u$ - and  $v$ -type particle properties in Hilbert space. The electron motion in orbit at positions 0 to 8 is attained in the form, *electron*  $\rightarrow$  *positron*  $\rightarrow$  *electron* at  $720^\circ$  rotation within a classical spherical rotation of  $360^\circ$  and this somewhat mimics the Dirac belt trick [5] of Dirac fermion. Maximum twist from the torque of the BOs is attained at position 4 for a positron of high energy and the unfolding process restores the electron at position 8 or 0 in a repetitive process. In this way, both local realism and entanglement are assumed by the electron such as shown for a double slit experiment (Fig. 4;

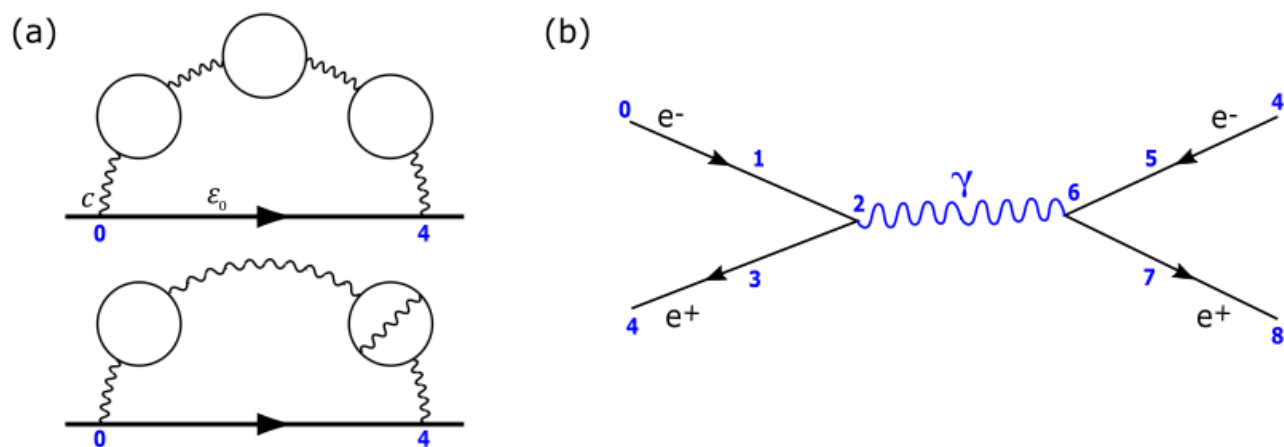


**Figure 5. Feynman diagrams of electron-positron pairings.** (a) Orthogonal relationship of  $\mathbf{E}$  and  $\mathbf{B}$  for eight-order Feynman diagrams of the electron-self interaction within a hemisphere [32]. This is somehow relatable to Fig. 4. For example, the arrowed horizontal line represents the actual electron path, which

acquires electron-positron pair. Wavy lines are virtual photons with the circles assigned to assumed precessing stages of the MP field in Hilbert space. The applicability of the physical constants like,  $\varepsilon_0$  and  $c$  are demonstrated, while  $\hbar$  and  $e^2$  are provided in Fig. 4 with respect to the electron path. These processes are applicable to a generic Feynman diagram (b).

*Postulate 5).* Multiple slits are envisioned for the electron path. Translation of the hemisphere to multi-order Feynman diagrams (Fig. 5a and b) incorporates the physical constants like fine-structure constant,  $\alpha$ , vacuum permittivity,  $\varepsilon_0$ , reduced Planck constant,  $\hbar$  and lightspeed,  $c$ , where the value of the electron charge is calculated, i.e.,  $e^2 = 4\pi\varepsilon_0\hbar c\alpha$ . In this way, the reciprocal of the mystical dimensionless value [33, 34],  $\alpha$  as  $1/137$  is ably accounted for, which otherwise cannot be explained by QTF application the conventional way. The antisymmetric product of one-particle solutions [35] of the electron is given by,

$$\psi(x_1, x_3) = \varphi_1(x_1)\varphi_3(x_3) - \varphi_1(x_3)\varphi_3(x_1). \quad (6a)$$

$$\hat{P}\psi(x_1, x_3) = \varphi_1(x_3)\varphi_3(x_1) - \varphi_1(x_1)\varphi_3(x_3),$$

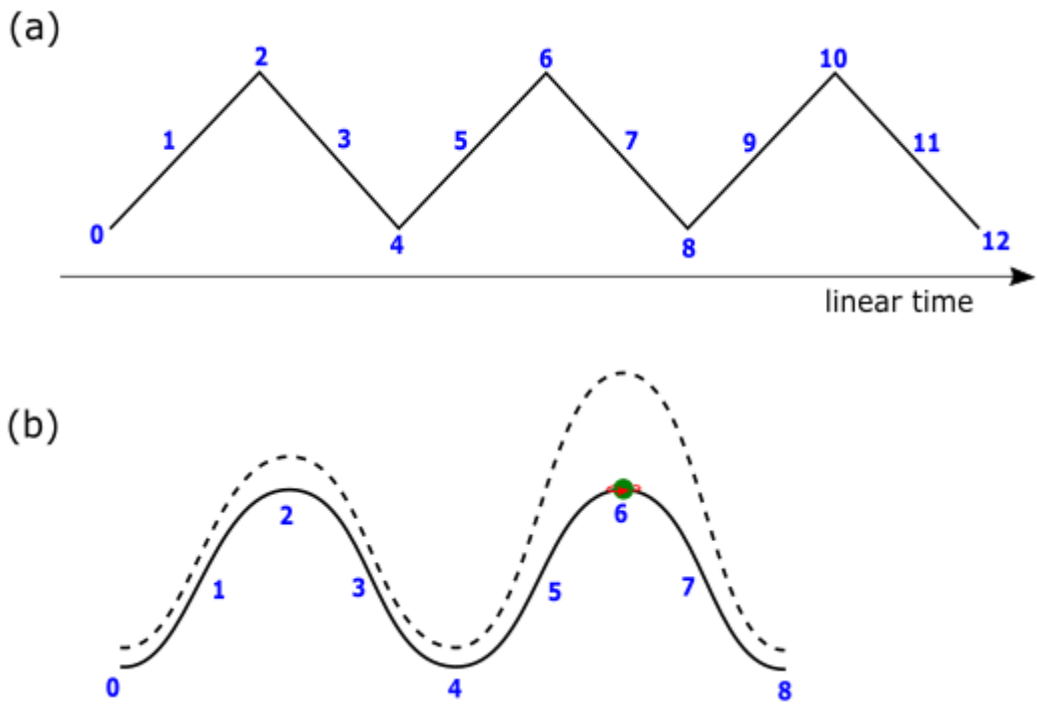
$$= -\psi(x_1, x_3). \quad (6b)$$

$\hat{p}$  is the probability operator for the Hermitian of the spin  $1/2$  property of Dirac matrices,  $\gamma^{1,3}$  (Fig. 4) by the reduction of the Dirac fermion [3, 4] of a four-component spinor field,  $i\gamma^0\gamma^1\gamma^2\gamma^3$ .  $\varphi$  is the spinor generated along the BOs into  $n$ -dimensions of Hilbert space either in outward direction from the precessing MP field or inward direction from the electron's orbit of time reversal to generate both  $u$ - and  $v$ -type particles (Fig. 4). Both are encased by the

configurations,  $\Omega$  of same magnitudes (Fig. 3). Equation 6b is reduced to,  $\pm\psi(1/2)$  at positions  $x_1, x_3$  with  $\pm 1$  equal to spherical polarization (Fig. 4; *Postulate 3*). Such intuition is consistent with experiments violating Bell’s inequality tests [36, 37] supposing multielectron are applicable to multiple MP fields (*Postulate 1*) and their interactions with photons could somehow correlate at a distance.

## 6. Implications – Generation of electromagnetic waves

How the electron or Dirac fermion accommodates electromagnetic field of linear time at observations is examined. In Fig. 6a, b and c, both the radial and angular distributions are given.





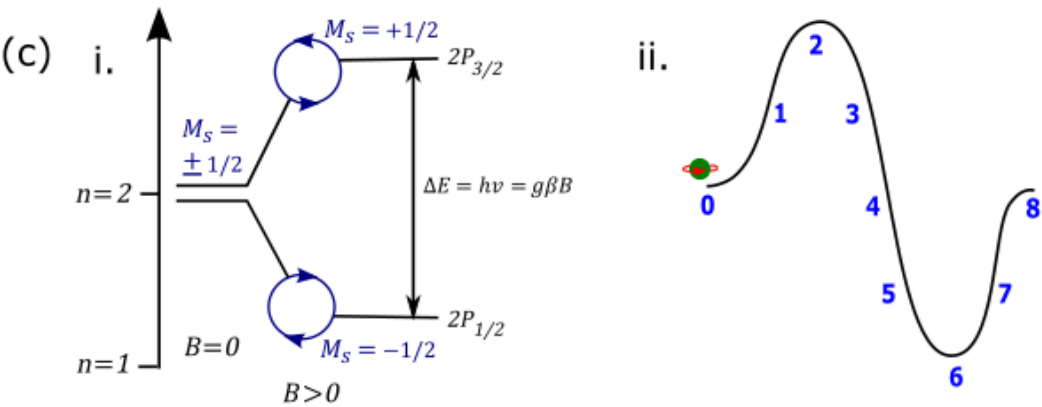


**Figure 6. Induction of electromagnetic waves from the MP model into space.** (a)  $\mathbf{B}$  assumed at positions 0 to 4 is accompanied by  $\mathbf{E}$  of a hemisphere at spherical rotation of  $180^\circ$  (e.g., Fig. 4). The numbered positions from 9 onwards repeat the process described by positions 0 to 8 of the MP model (see Fig. 1a and b). (b) Radial distribution of sinusoidal wave is energized by the presence of the electron (dotted wavy curve). The energy dissipation into space from external light interaction could resemble water waves losing energy into open space while the electron and hence, atom is conserved. (c) (i) In the presence of a weak external  $\mathbf{B}$ , the energization of the model from the ground state,  $n = 1$  at 0 position to the excited state,  $n = 2$  allows for the spin-orbit splitting to emerge from the degenerate BOs (Fig. 1b) such as for the 2P orbital noted for electron paramagnetic resonance [38]. (ii) Dirac belt trick. The electron is converted to a positron at position 4 and it is restored at position 8 or 0 (see also Fig. 2). The energy difference,  $\Delta E$  between the spins is proportional to the  $g$ -factor ( $g$ ) and Bohr magneton ( $\beta$ ). The selection rule,  $\Delta M_S = \pm 1$  is offered in Fig. 4.

The electron's presence energizes the electromagnetic waves projected along the intranuclear or  $z$ -axis with external light interactions without dislodging it from the atom. The orthogonality of Maxwell's electromagnetic waves is normalized to the intranuclear axis (e.g., Fig. 4 and 6b). The above interpretations can further extend to include Fourier transform, lamb shift and nuclear spin by assuming the applicability of the MP model to the nucleus. Further explanations are offered in

the Supplemental Material. The helicity of both the positron and electron is provided in Fig. 2. These explanations offer an alternative perspective to the Dirac fermion and hence, spin-orbit coupling splitting.

## 7. Conclusion

The MP model of 4D space-time for the hydrogen atom of Bohr model considered in this study is somehow able to transform the electron to Dirac fermion of a four-component spinor field. Its evolution with time is defined by Schrödinger  $\psi$  and this sustains local realism. The transformation of the electron to electron-positron pair during its orbit at more than lightspeed in both Euclidean and Minkowski space-times offers entanglement. These outcomes present an alternative perspective to spin-orbit coupling splitting from external light interactions. If considered, such findings could consolidate properly the fundamentals of the quantum state of matter from an alternative perspective using QFT application and they warrant further investigations.

## Competing financial interests

The author declares no competing financial interests.

## References

1. M. Pawłowski et al. Information causality as a physical principle. *Nature* 461(7267), 1101-1104 (2009).
2. J. Henson. Comparing causality principles. *Stud. Hist. Philos M. P.* 36(3), 519-543 (2005).
3. M. E. Peskin & D.V. Schroeder. *An introduction to quantum field theory*. Addison-Wesley, Massachusetts, USA (1995).
4. L. Alvarez-Gaumé & M. A. Vazquez-Mozo. Introductory lectures on quantum field theory. *arXiv preprint hep-th/0510040* (2005).
5. L. S. Weiss et al. Controlled creation of a singular spinor vortex by circumventing the Dirac belt trick. *Nat. Commun.* 10(1), 1-8 (2019).
6. Z. K. Silagadze. Mirror objects in the solar system?. *arXiv preprint astro-ph/0110161* (2001).
7. Z. Y. Li. Elementary analysis of interferometers for wave—particle duality test and the prospect of going beyond the complementarity principle. *Chin. Phys. B* 23(11), 110309 (2014).
8. M. Rabinowitz. Examination of wave-particle duality via two-slit interference. *Mod. Phys. Lett. B* 9(13), 763-789 (1995).
9. E. Nelson. Derivation of the Schrödinger equation from Newtonian mechanics. *Phys. Rev.* 150(4), 1079 (1966).

10. C. Rovelli. Space is blue and birds fly through it. *Philos. Trans. Royal Soc. Proc. Math. Phys. Eng.* 376(2123), 20170312 (2018).
11. D. H. Perkins. Proton decay experiments. *Ann. Rev. Nucl. Part. Sci.* 34(1), 1-50 (1984).
12. H. Sun. Solutions of nonrelativistic Schrödinger equation from relativistic Klein–Gordon equation. *Phys. Lett. A* 374(2), 116-122 (2009).
13. S. Oshima, S. Kanemaki & T. Fujita. Problems of Real Scalar Klein-Gordon Field. *arXiv preprint hep-th/0512156* (2005).
14. S. D. Bass, A. De Roeck & M. Kado. The Higgs boson implications and prospects for future discoveries. *Nat. Rev. Phys.* 3(9), 608-624 (2021).
15. S. P. Yuguru. Unconventional reconciliation path for quantum mechanics and general relativity. *IET Quant. Comm.* 3(2), 99–111 (2022).
16. A. Almasi et al. New limits on anomalous spin-spin interactions. *Phys. Rev. Lett.* 125(20), 201802 (2020).
17. C. N. Yang & R. Mills. Conservation of isotopic spin and isotopic gauge invariance. *Phys. Rev.* 96, 191 (1954).
18. D. J. Gross. Nobel lecture: The discovery of asymptotic freedom and the emergence of QCD. *Rev. Mod. Phys.* 77(3), 837 (2005).
19. P. Higgs. Spontaneous symmetry breakdown without massless bosons. *Phys. Rev.* 145, 1156 (1966).
20. S. Weinberg. Implications of dynamical symmetry breaking. *Phys. Rev. D* 13, 974 (1976).
21. N. Straumann. Wolfgang Pauli and modern physics. *Space Sci. Rev.* 148(1), 25-36 (2009).

22. N. Arkani-Hamed et al. Solving the hierarchy problem with exponentially large dimensions. *Phys. Rev. D* 62(10), 105002 (2000).
23. D. Howard. Who invented the “Copenhagen Interpretation”? A study in mythology. *Philos. Sci.* 71(5), 669-682 (2004).
24. V. B. Morozov. A note on the equivalence principle applicability to the general theory of relativity. *arXiv preprint arXiv:1404.3083* (2014).
25. J. D. Barrow & J. Levin. Twin paradox in compact spaces. *Phys. Rev. A* 63(4), 044104 (2001).
26. A. M. Nobili & C. M. Will. The real value of Mercury's perihelion advance. *Nature* 320(6057), 39-41 (1986).
27. E. Da Cunha et al. On the effect of the cosmic microwave background in high-redshift (sub-) millimeter observations. *The Astrophys. J.* 766(1), 13 (2013).
28. R. Clausius. The mechanical history of heat. Chapter 9. pp 365. J. Van Voorst (1867).
29. S. B. McKagan, K. K. Perkins & C. E. Wieman. Why we should teach the Bohr model and how to teach it effectively. *Phys. Rev. Phys. Edu. Res.* 4(1), 010103 (2008).
30. P. Atkins & J. de Paula. *Physical Chemistry*. 9<sup>th</sup> Edition. Oxford University Press, New York (2010).
31. D. J. Wineland. Nobel lecture: Superposition, entanglement, and raising Schrödinger's cat. *Rev. Mod. Phys.* 85(3), 1103 (2013).
32. Examples of 8-order Feynman diagrams for electron propagation, Wikimedia Commons <https://en.wikipedia.org/wiki/Image:EighthOrderMagMoment.svg> (Accessed online on 24 November, 2022).

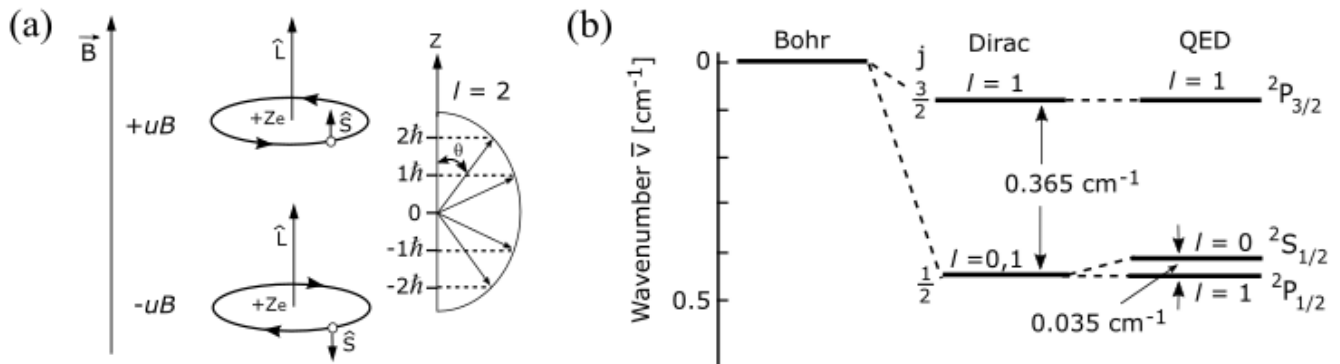
33. H. Kragh. Magic number: A partial history of the fine-structure constant. *Arch. Hist. Exact Sci.* 57(5), 395-431 (2003).
34. M. A. Sherbon. Fundamental nature of the fine-structure constant. *Int. J. Phys. Res.* 2(1), 1-9 (2014).
35. A. Szabo & N. S. Ostlund. *Modern quantum chemistry: introduction to advanced electronic structure theory*. Courier Corporation, Massachusetts, USA (1996).
36. A. Aspect, P. Grangier & G. Roger. Experimental realization of Einstein-Podolsky-Rosen-Bohm Gedanken experiment: a new violation of Bell's inequalities. *Phys. Rev. Lett.* 49(2), 91 (1982).
37. J. W. Pan et al. Experimental entanglement swapping: entangling photons that never interacted. *Phys. Rev. Lett.* 80(18), 3891 (1998).
38. J. A. Weil & J. R. Bolton. *Electron paramagnetic resonance: elementary theory and practical applications*. John Wiley & Sons (2007).
39. H. Haken & H. C. Wolf. *The physics of atoms and quanta: introduction to experiments and theory* (Vol. 1439, No. 2674). Springer Science & Business Media (2005).
40. G. Gabrielse et al. New determination of the fine structure constant from the electron  $g$  value and QED. *Phys. Rev. Lett.* 97(3), 030802 (2006).
41. D. Hanneke et al. Cavity control of a single-electron quantum cyclotron: Measuring the electron magnetic moment. *Phys. Rev. A* 83(5), 052122 (2011).
42. J. C. Lindon, G. E. Tranter & D. Koppenaal. *Encyclopedia of spectroscopy and spectrometry*. Academic Press (2016).

## Supplemental Material

Based on the transformation of the electron to Dirac fermion, alternative interpretations are offered on the basics of spin-orbit coupling splitting. This is done to demonstrate the compatibility of QFT application to the MP model of 4D space-time.

### Spin-orbit coupling of the electron

Diagonal coupling of rotating BOs and  $\vec{L}$  produces intrinsic properties of  $\vec{J}$  or the spinor in units of  $\hbar$  (Supplemental Fig. 1a). This is related to the reduction of Dirac fermion of four-component spinor field to spin  $\pm 1/2$  states (Fig. 1b and Supplemental Fig. 1b). The pair of light-cones is of time invariant to the helicity of the model (Fig. 2). From zero-point energy at position 0, energy absorption activates the BOs from  $n = 1$  to  $n = 2$  for the spin-orbit coupling of 2P orbital (Fig. 6c(i) and (ii)) in Minkowski space-time (Fig. 1b). This relates to Dirac spinor and hence, the lamb shift and are rigorously pursued by the theory of quantum electrodynamics. Somehow, both are applicable to the MP model, where renormalization appears to be heuristic in principle (e.g., Fig. 5a and b; *Postulate 4*). Thus, at position 1 of Minkowski space-time, the total angular momentum,  $\vec{J} = l \pm \frac{1}{2}$ , provides the values,  $\frac{3}{2}$  and  $\frac{1}{2}$  for  $p$  orbital at  $n = 2$ ,  $l = 1$  and this relates to the degenerate states of BOs. Similarly, the Clebsch–Gordon series for the total orbital angular moment,  $\vec{L} = \sqrt{l(l+1)}\hbar$  and total spin,  $\vec{S} = \sqrt{s(s+1)}\hbar$  are applicable to the BOs of  $n$ -



**Supplemental Figure 1. Spin-orbit coupling splitting [30, 39].** (a) In the presence of a weak external magnetic field,  $\vec{B}$ , its dipole moment,  $uB$  of classical Bohr magneton exerts corresponding response from the electron's dipole moment. The combined dipole is,  $u_z = u_B + u_l$ , with  $u_l$  equal to  $\vec{j}$  and  $\vec{j} = l + 1/2$  (e.g., Fig. 1b). The electron's orbit in Hilbert space is quantized,  $\hbar$  (e.g., Fig. 4) and is aligned perpendicularly to its magnetic momentum,  $m$  at the center. (b) When the electron and the MP field dipole moments, i.e.,  $\hat{S}$  and  $\hat{L}$  respectively are aligned to  $\vec{B}$ ,  $2P_{3/2}$  is produced at high energy such as for a positron (Fig. 6c(i)). In the anticoupling process with  $\hat{S}$  in the opposite direction,  $2P_{1/2}$  for the electron is assumed at a slightly lower energy than  $2S_{1/2}$  for the lamb shift. This is attributed to the degenerate states of BOs. The pursuits of spin-orbit coupling splitting become more complex from the Bohr model to Dirac field theory followed by quantum electrodynamics.

dimensions. For example, the magnitude [30],  $\vec{j} = \vec{L} + \vec{S}$  is assumed by a triangulated geometry at positions 0, 2 and 3. The shift in position is dictated by Einsteinian gravity against forward time of a clock face (Fig. 1b; *Postulate 1*). The lamb shift refines the value of the fine-structure constant,  $\alpha$  to about less than 1 part in a billion [40] and it quantifies the gap between the fine structure of the hydrogen spectral lines. It is a measure of the strength of the electron and its interaction with the electromagnetic field by the relationship [33, 34],



$$a = \frac{e^2}{4\pi\epsilon_0}. \quad (7)$$

In high-energy physics, a nondimensional system is used with the boundary,  $\epsilon_0 = c = \hbar = 1$  (see also *Postulate 2*), so Equation 7 is reduced to the form,

$$a = \frac{e^2}{\hbar c} \approx \frac{1}{137.036}. \quad (8)$$

In this study,  $\alpha$  is naturally accounted for by the MP model as mentioned earlier (e.g., Fig. 4, 5a and b). It provides powers to the perturbative expansion of the anomalous dipole moment of the electron with respect to its  $g$ -factor in the form,

$$g_e = 2 \left( 1 + \frac{a}{2\pi} + \dots \right). \quad (9)$$

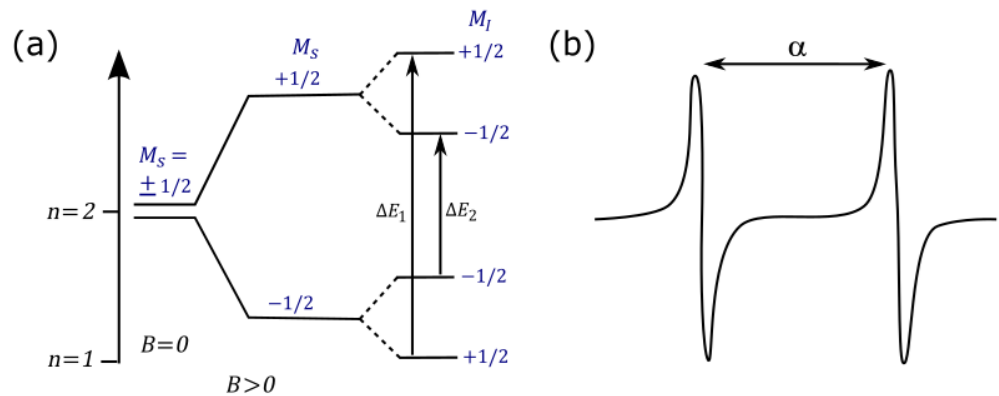
Equation 9 describes how the electron undergoes  $720^\circ$  rotation to resume its original position or is twice faster (*Postulate 5*) than a classical spherical rotation at  $360^\circ$  in continuum mode (Fig. 1a). The general consensus to the predicted and measured  $g$ -factor of the electron is calculated to about 10 decimal points [41]. The relationship between the generated magnetic moment,  $u_s$  and  $g$ -factor is given by,

$$u_s = g_e \frac{u_B}{\hbar} s, \quad (10)$$

where  $s$  is the intrinsic spin property of the electron and  $u_B$  is a classical Bohr magneton (Fig. 6c(i) and Supplemental Fig. 1b). Unlike a rotating classical object, the electron's spin and angular momentum are applicable in Minkowski space-time (Fig. 1b). Other related themes that can perhaps be explored in a similar manner include Coulomb interactions, Rydberg constant, Compton scattering and so forth.

### Spin-orbit coupling at the nucleus

By extending the electron spin-orbit coupling (Fig. 6c(i) and (ii)), this can accommodate the gauge symmetry,  $SU(3)$  flavor octet ( $J = 1/2$ ) and its decuplet ( $J = 3/2$ ) of the weak nuclear isospin for baryonic matter of quarks. Explanations for Dirac fermion are offered above with respect to corresponding  $J$  values so these could also become applicable to quarks. Such a



**Supplemental Figure 2. Spin-orbit coupling splitting [42].** (a) The spin-orbit coupling doublet state incorporates both the electron and the nuclear magnetic spin,  $M_I$  (see also Fig. 6c(i) and (ii)). (b) Hyperfine coupling constant,  $\alpha$  of the electron paramagnetic resonance spectra possibly links the MP models between the atom and the nucleus in a possible multiverse scenario (*Postulate 4*).

relationship can be established by the magnetic spin of both the electron and the nucleus (Supplemental Fig. 2a and b). The hyperfine constant,  $\alpha$  offers the energy difference between them. With quark confinement, the selection rule for the nuclear magnetic spin is,  $\Delta M_I = 0$  unlike the electron, where  $\Delta M_S = \pm 1$  (e.g., Supplemental Fig. 2a). Thus, for the electroweak nuclear decay like beta decay,  $n^{\circ} \rightarrow p + W^- \rightarrow uud + e^- + \bar{\nu}$ , it reinforces the MP models for both the quark and electron at different energy scales (*Postulate 4*). The transition between them can somehow translate to either neutrinos at  $720^{\circ}$  rotation or  $360^{\circ}$  rotation for antineutrinos in Hilbert space (see also Fig. 5a and b). Mass acquisition is then obtained by oscillation process and is somewhat comparable to Higgs mechanism (e.g., Fig. 3). These interpretations can constrain the free parameters of the Standard Model of non-abelian in terms of particle masses and mixing angles in both Euclidean (Fig. 1a) and Minkowski space-times (Fig. 1b) from an alternative perspective. The color change of charges for gluons would then resemble the photons interceptions of the spherical rotation of the electron propagation path (e.g., Fig. 5a and b). The three generations of the quarks and leptons would appear as a function of increasing mass in onion-like structure of the MP models analogous to the spin-orbit coupling triplet state of Zeeman effect. Whether the model can be extended to incorporate the principles of general relativity remains a possibility as implied in a recent study [15] (*Postulate 4*). Some of those inferred in the Conceptualization process of the MP model (Section 3) include both Euclidean and Minkowski space-times, the equivalence principle, inertia frame of reference, Einsteinian gravity, gravitational time dilation, gravitational lensing and perihelion precession. However, this does not accommodate quantum gravity, gravitational waves or black holes.